Mitigation of Dead-Time Effects on Transient DC Bias Elimination in Dual Active Bridge Link Current

MK Kharabela Mohanta, Dipankar De, Silpashree Sahu
School of Electrical Sciences
Indian Institute of Technology Bhubaneswar
Jatni, Odisha-752050, India
email: dipankar@iitbbs.ac.in

Alberto Castellazzi
Faculty of Engineering
Kyoto University
18 Gotanda-cho, Yamanouchi
Ukyo-ku, Kyoto, Japan, 615-8577
email: alberto.castellazzi@kaus.ac.jp

Keywords

≪Dual Active Bridge (DAB)≫, ≪Dead-time≫, ≪Converter control≫, ≪Compensation≫

Acknowledgement

This work is supported by Department of Science and Technology (DST), India under project grant ECR/2017/001079.

Abstract

Transient DC bias elimination in the link current of the dual active bridge DC-DC converter under power transients including dead-time effect is investigated in this paper. When a power change command is given to a dual active bridge, the modulation instants should be adjusted in an adequate manner in order to avoid over current during transients. The paper summarizes the adverse effect of the dead-time in applying DC-bias elimination techniques by dividing the entire operating region into six different zones based on operating phase angles and in terms of dead-time. An improved compensation method (based on pre-, post- transition current waveform computation) to mitigate the dead-time effect is suggested. A detailed mathematical analysis is carried out to select the suitable switching instants. The proposal is demonstrated through simulation studies and through experimental verification.

Introduction

One of the main challenges in designing modulator for Dual Active Bridge DAB converter [1, 2] is the transient DC bias current through the link inductance. The DC bias elimination technique is reported in [3–9] where extensive simulation and/or experimental results were presented to reduce the unwanted current stress on the power converter components. On the other hand, different optimization techniques are reported in the literature for DAB converter to improve its steady state performance. The optimization techniques (reported in [10, 11]) explain about the RMS link current and reactive power optimization respectively. In this work the optimization

method for steady state performance is combined with the transient DC bias elimination algorithm. The second concept that this paper focuses is the effect of dead-time on the transient DC-bias elimination method. There are a good number of reported works in the literature to investigate and compensate the effect of dead-time to improve the performance of the dual active bridge converter [12–14]. In [15], a technique to eliminate DC bias current including dead-time is reported. A DC bias current elimination technique (with accurate computation of intermediate phase shifts during transients) is proposed in this work to mitigate the effect of dead-time and the corresponding mathematical/analysis is investigated. The proposed method unlike the previously reported method considers adverse effect on the dead time especially when the switching takes place closed to zero link current or link current reaches to zero during dead-time. The entire operating zone is classified in six sub-zones based on operating phase angles and in terms of dead-time (not in the form of power directly). The verification of the proposed concept is presented along with an optimization technique and the improvements achieved by this method are highlighted.

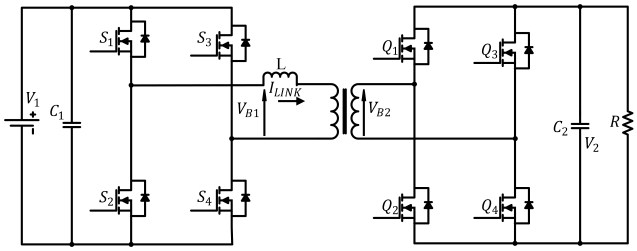

Fig. 1: Dual active bridge converter topology connected in power circulation mode

Transient DC Bias Without Dead-time Effects

Fig. 1 shows the basic circuit diagram of dual active bridge connected with source V_1 at the input side and load resistance R at the output. Let us consider a basic transient DC bias control technique to start with ignoring the effect of dead-time. The operation of dual active bridge usually has two phase shifts namely, the phase shift between the two full bridges (ϕ) and one inner phase shift (α) in the primary bridge (between the two legs of the converter). Hence, the transient operation can be divided into two zones based on $\phi < \alpha$ (zone-1) and $\alpha < \phi$ (zone-2).

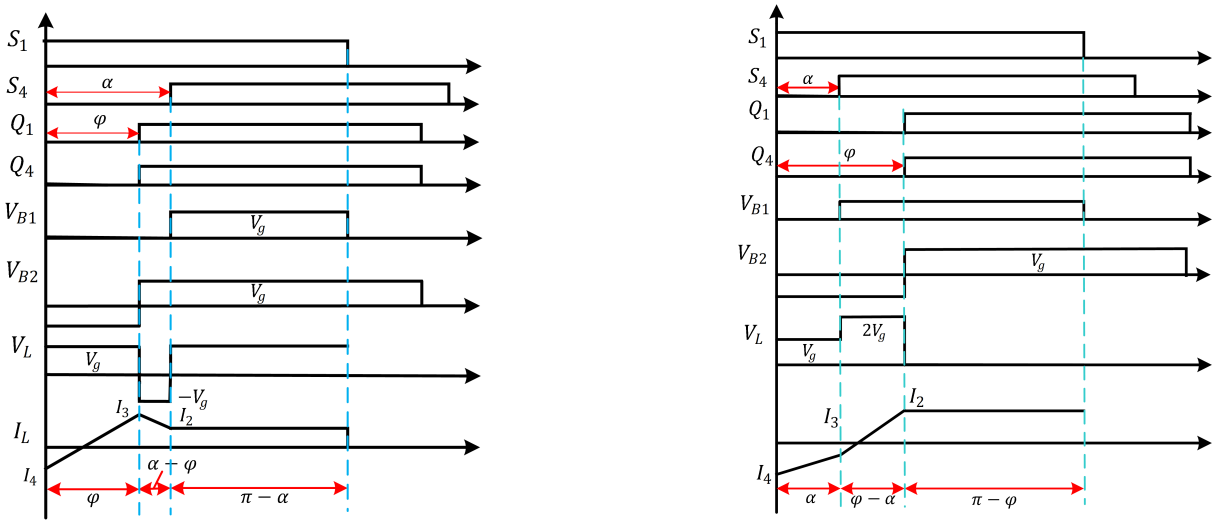

Fig. 2: Waveforms of zone-1 (a) and Waveforms of zone-2 (b)

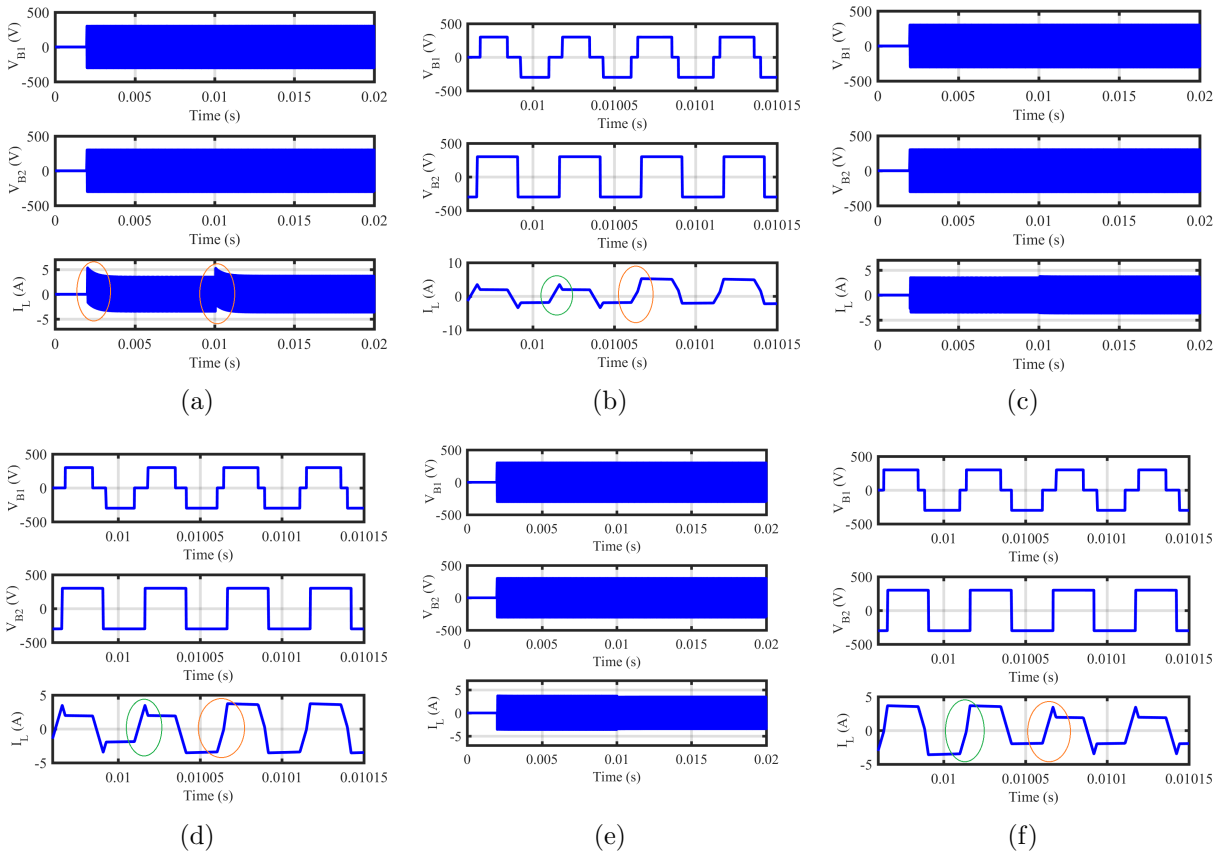

Fig. 3: Simulated Waveform for transition from Zone-1 (400W) to Zone-2 (800W): (a) complete transitions (b) zoomed at the power transition instant without DC-bias Elimination (without considering the effect of dead-time); Simulated Waveform for transition from Zone-1 (400W) to Zone-2 (800W): (c) complete transitions, (d) zoomed at the power transition instant with DC-bias Elimination techniques (without considering the effect of dead-time); Simulated Waveform for transition from Zone-2 (800W) to Zone-1 (400W): (e) complete transitions, (f) zoomed at the power transition instant with DC-bias Elimination techniques (without considering the effect of dead-time)

Fig. 2 shows the various typical waveforms such as primary voltage, secondary voltage, link voltage and link current for zone 1 (top figure) and for zone 2 (bottom figure). As the number of zones are two, there are total four possible combination of transitions possible when there is a transient change in the power reference. Fig. 3(a) shows the simulated result of transient DC bias current without any additional DC-bias elimination technique for zone 1 to zone 2 transition. The power transition instant is shown by the arrow mark and it can be observed that there is some DC bias in the link current at the power transition instant Fig. 3(b) zoomed at the transient instant.

Transient DC Bias Control Without Dead-time Effects

A transient DC-bias elimination technique is used to remove the DC Bias current during the transient process for all four cases. The main objective is that the current during its transition from one zone of operation to another zone should complete within half switching cycle (with the starting and end corner points of the link current as the steady state values of the respective zones). The mathematical description of one of the transitions (zone 1 to zone 2) is given in the following. Let, I_{41} is the negative steady state point for the pre-transition operating point for power P_1 and I_{22} is the positive steady state point for the post transition operating point for

power P_2.

$$I_{41} = \frac{V_g T_s}{2L\pi}(-\phi_1 + \frac{\alpha_1}{2});\;\; I_{22} = \frac{V_g T_s}{2L\pi}(\phi_2 - \frac{\alpha_2}{2}) \tag{1}$$

The transient equations can be obtained by assuming the transitions are taking place in zone-2 and intermediate corner point has 50% value of I_{41} ($I_{32m} = x \times I_{41}$ with $x = 0.5$):

$$I_{41} + \frac{V_g T_s}{2L\pi}(\alpha_m) = I_{32m};\;\; I_{32m} + (\phi_m - \alpha_m)\frac{-2V_g T_s}{2L\pi} = I_{22} \tag{2}$$

Where, I_{31m} is the intermediate value and (α_1,ϕ_1), (α_2,ϕ_2) and (α_m,ϕ_m) are the pre transition, post transition and intermediate (for the transition period of half cycle) phase shifts respectively. Solving the above equations, we can obtain the intermediate phase shift needed for a smooth and DC bias free transition.

$$\phi_m = \frac{I_{22}}{2k} + \frac{I_{41}}{4k};\;\; \alpha_m = \frac{I_{41}}{2k} \tag{3}$$

Here, $(V_g T_s)/(2L\pi) = k$. It can be noted that the condition of having transition points in zone-2, $\alpha_m < \phi_m$ or $I_{22} > 0.5I_{41}$ should be satisfied. Otherwise, the intermediate angle values are to be determined assuming the the transitions are taking place in zone-1. Alternatively, the fraction x can be chosen such that it satisfies the zone-2 conditions. Fig. 3(c) shows the simulated waveforms for the transition from zone-1 to zone-2. The waveforms at the instant of power transients are zoomed and are shown Fig. 3(d). It can be clearly observed that during the transitions no additional DC bias present. An optimization block takes the power command P and a fraction F for the optimization (similar to the method that reported in [16–18]). The details of the optimization block will be explained in the subsequent sections. Similarly, Fig. 3(e), (f) show the simulated waveforms for the transition from zone-2 to zone-1.

Effect of Dead-time on DC Bias Current

With the incorporation of dead-time each zone can further be subdivided into 3 different sub-zones depending on link current direction and magnitude. These zones are shown in Table I. Case-A, Case-B and Case-C are the 3 sub-zones of zone-2 and Case-D, Case-E and Case-F are the 3 sub-zones of zone-1. Table. I provides the conditions or relationship between various phase angles for different cases/zones. Fig. 4 shows the effect of dead time on the link current corner points at various zones (Mode-A, Mode-B, Mode E are shown) and it can be seen that if the technique is not updated accordingly the performance of the DC bias elimination get affected and an unwanted deviation appears in the link current during the transients (as it can be seen from Fig. 5(a), (b) where case-A to case-B transition is shown without any dead-time compensation). The expression of the corner point current magnitudes at Mode-A, Mode-B, Mode E (as in Fig. 4) are summarized as follows:

- Case-A:

$$I_3 = \frac{V_g T_s}{2L\pi}(\phi - \frac{\alpha}{2}) = -I_1;\;\; I_2 = \frac{V_g T_s}{2L\pi}(-\phi - 1.5\alpha) \tag{4}$$

- Case-B:

$$I_3 = \frac{V_g T_s}{2L\pi}(\phi - \frac{\alpha}{2} - \frac{D_T}{2}) = -I_1;\;\; I_2 = \frac{V_g T_s}{2L\pi}(-\phi - 1.5\alpha + 1.5D_T) \tag{5}$$

- Case-E:

$$I_3 = \frac{V_g T_s}{2L\pi}(\phi - \frac{\alpha}{2} - \frac{D_T}{2}) = -I_1;\;\; I_2 = \frac{V_g T_s}{2L\pi}(\frac{\alpha}{2} - \frac{D_T}{2}) \tag{6}$$

Table I: Conditions of Different Cases

Zones	Conditions	Parameters	Specifications
A	$\phi > \alpha,\ -\phi + 1.5\alpha < -2D_T$	V_1	300 V
B	$\phi > \alpha,\ -\phi + 1.5\alpha > -0.5D_T$	V_2	300 V
C	$\phi > \alpha,\ -2D_T < -\phi + 1.5\alpha < -0.5D_T$	Switching Frequency	20 kHz
D	$\alpha > \phi,\ -\phi + 0.5\alpha < -1.5D_T$	Inductor (L)	360 μH
E	$\alpha > \phi,\ -\phi + 0.5\alpha > -D_T$	Dead time	1 μs
F	$\alpha > \phi,\ -1.5D_T < -\phi + 0.5\alpha < -D_T$	Transformer	1 : 1

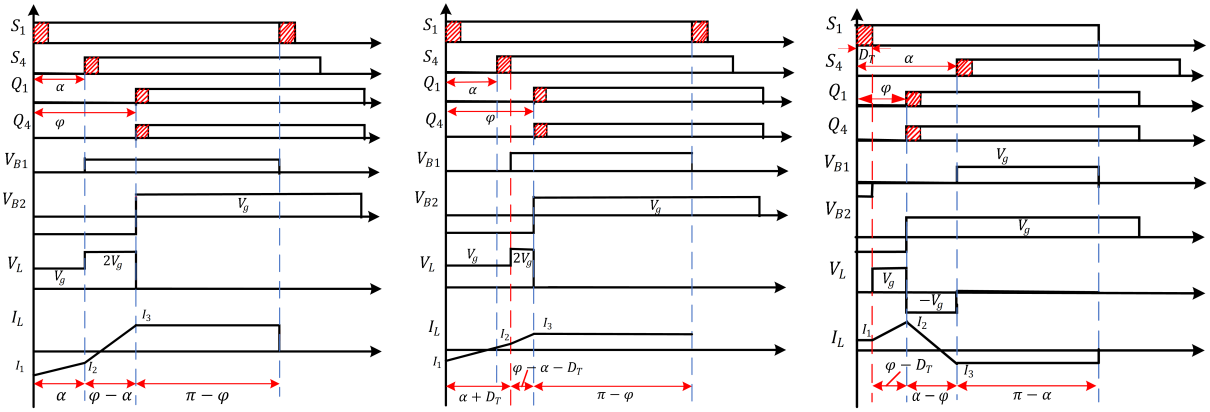

(a) (b) (c)

Fig. 4: Illustrative wave forms for current corner points considering the effect of dead-time (a) Case-A, (b) Case-B, (c) Case-E

Proposed Mitigation Techniques

Mathematical Expressions for Different Zones

The modified values of the phase shift can be adjusted by incorporating the effect of dead time in the computation. The mathematical expressions for two cases are shown in this section even though the implementation involves all the possible configurations. The transition from Case-A to Case-B can be described as follows. The transient equations in this case can be written as:

$$I_{1A} + \frac{V_g T_s}{2L\pi}(\alpha_{mA}) = I_{mA};\ \ I_{mA} + \frac{2V_g T_s}{2L\pi}(\phi_{mA} - \alpha_{mA}) = I_{3B} \tag{7}$$

Where, I_{1A} is the negative steady state corner point of the link current with the system is operating in Case-A condition and I_{3B} is the positive steady state corner point of the link current with the system is operating in Case-B condition.

$$I_{1A} = -\frac{V_g T_s}{2\pi L}(\phi_1 - \alpha_1);\ \ I_{3B} = \frac{V_g T_s}{2\pi L}\left(\phi_2 - \frac{\alpha_2}{2} - \frac{D_T}{2}\right) \tag{8}$$

I_{mA} is the intermediate operating point. By solving above equations with assumption $I_{mA} = 0.5I_{1A}$ (ensures the transition interval within zone-A), we get,

$$\alpha_{mA} = \frac{I_{1A}}{k} - \frac{I_{mA}}{k} = 0.5\frac{I_{1A}}{k};\ \ \phi_{mA} = \frac{I_{3B}}{2k} - \frac{3I_{mA}}{2k} + \frac{I_{1A}}{2k} = \frac{I_{3B}}{2k} + \frac{I_{1A}}{4k} \tag{9}$$

Table I shows the power circuit parameters used for simulation/experiments and different power values considered in different zone for validation of the proposed concepts. Fig. 5(c), (d) show

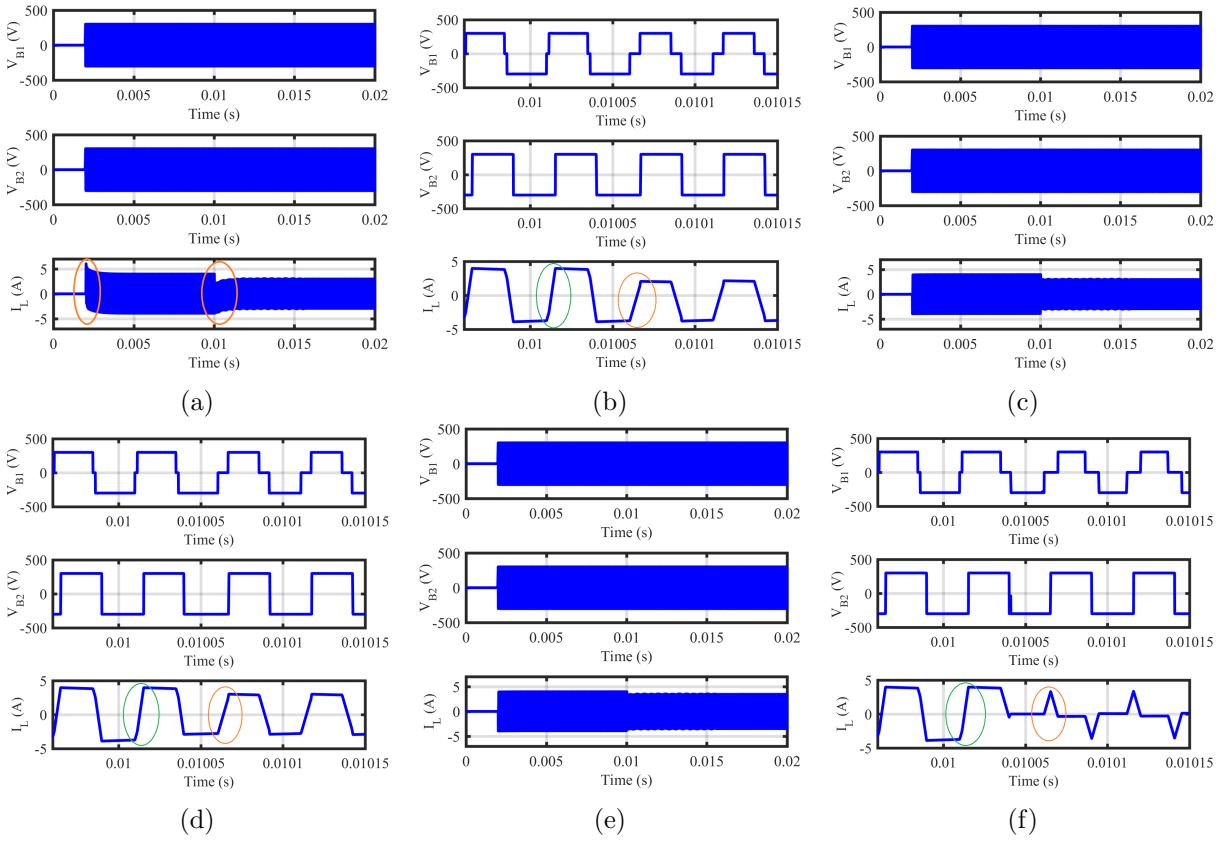

Fig. 5: Simulated Waveform for transition from Case-A to Case-B: (a) complete transitions. (b) zoomed at the power transition instant with DC-bias Elimination techniques (no compensation associated with dead-time); Simulated Waveform for transition from Case-A to Case-B: (c) complete transitions, (d) zoomed at the power transition instant with the proposed DC-bias Elimination techniques; Simulated waveform for Transition from Case-A to Case-E (e) complete transitions, (f) zoomed at the power transition instant with the proposed DC-bias Elimination techniques

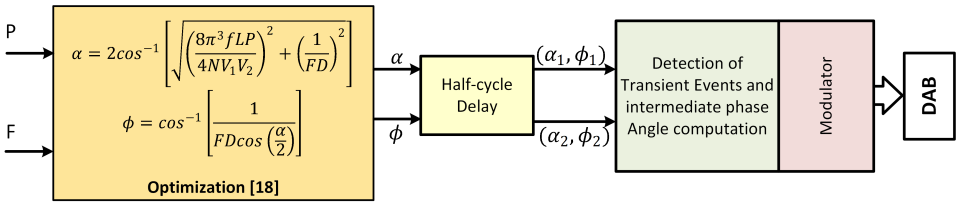

Fig. 6: Complete Control Diagram for Modified for DC Bias Current Elimination

the transient result where there is a transition from Case-A to Case-B. The power transition is made at 0.01s and it can be observed that with proposed algorithm the dead time does not affect the link current during transients. The encircled portion in the figure indicates the two steady state transients before and after the power transition.

Similarly, for the transition from A to E, the corner points in each zone can be obtained as,

$$I_{1A} = \frac{V_g T_s}{2L\pi}(-\phi_1 + \frac{\alpha_1}{2}); \quad I_{3E} = \frac{V_g T_s}{2L\pi}(\phi_2 - \frac{\alpha_2}{2} - \frac{D_T}{2}) \tag{10}$$

The transient equation and the phase shift angles by taking α_m is equal to ϕ_m can be written

as

$$I_{1A} + \frac{V_g T_s}{2L\pi}(2\phi_m - \alpha_m - D_T) = I_{3E};\ \ \alpha_m = \phi_m = \frac{I_{3E}}{k} - \frac{I_{1A}}{k} + D_T \tag{11}$$

Fig. 5(e), (f) show the transient result where there is a transition from Case-A to Case-E with the dead-time compensation logic.

Complete Block Diagram with Modified DPS for DC Bias Elimination

Fig. 6 summarizes the complete block diagram of the proposed Modified DPS for DC Bias current elimination along with optimization block. This optimization ensures improved performance of the converter for given loading condition. The first step is to get the optimized α and ϕ value by taking power (P) and F as input as described in [18]. The power (P) is obtained from the output from DC voltage controller or it can be set to a particular value for a specified power transfer from input to output side. In the optimization block, by varying F different optimization in DAB performance can be achieved. For the minimization of fundamental component of link RMS current, $F = 1$ and for minimization of the fundamental component of reactive power flowing back to source, $F = 2$ [18]. D is the voltage ratio of the dual active bridge converter converter. After obtaining α and ϕ, these angles are passed through a delay block (half the switching period) to detect any power transient command. Once the α_1, α_2, ϕ_1 and ϕ_2 values are obtained, in case of any transition the zone of operation (the previous zone and the next zone) is detected first and then, α_m and ϕ_m are computed for DC bias elimination as discussed in the previous section.

Experimental Results

In order to verify the concept experimentally, the experimental lab prototype was built and the experimental set-up is shown in Fig. 7(a). The control signals are generated using digital signal controller TMS320F28335. A 1:1 HF transformer having 46 turns in both primary and secondary sides (E65/32/27 Ferrite Core) is used in the set-up. The DAB is connected in the circulating mode configuration, which circulates power in 300 V DC bus. The experimental results with proposed method with a transition from case-A 880W to case-B 730W, from case-B 730W to case-A 880W, from Case A 880W to Case E 50W are depicted respectively in Fig. 7(b), Fig. 7(c), Fig. 7(d). These figures show that the instant power change command (in channel-1) and the high frequency link current for the DAB converter (in channel-2). The instant of transition (of the power) within half the switching period are highlighted in these figures. The results show a smooth transition at power change. It can be noted that due to the computation of the pre-transient and post-transient instants (current corner points) and the required intermediate phase shift there is a one switching period delay in the execution of the transient events.

Conclusions

This work presents the effect of dead time on the transient DC-bias in the link current of DAB converter and a novel DC bias elimination technique is proposed incorporating the effect of dead time. The transitions between different zones are analysed mathematically. The expressions of various switch timings including the effect of dead time is derived based on different zones of operation in the DAB operation. The detailed simulation studies and experimental results are presented in the selected cases including the effect of unavoidable dead-time effects. The presented simulation and experimental results show the effectiveness of the (DAB link current) DC Bias elimination method. The immediate future work lies in extending the above study for any possible transition.

References

[1] Mi C., Bai H., Wang C., and Gargies S.: Operation, design and control of dual H-bridge based isolated bidirectional DC-DC converter, IET Power Electronics, Vol.1, No. 4, pp. 507-517, March

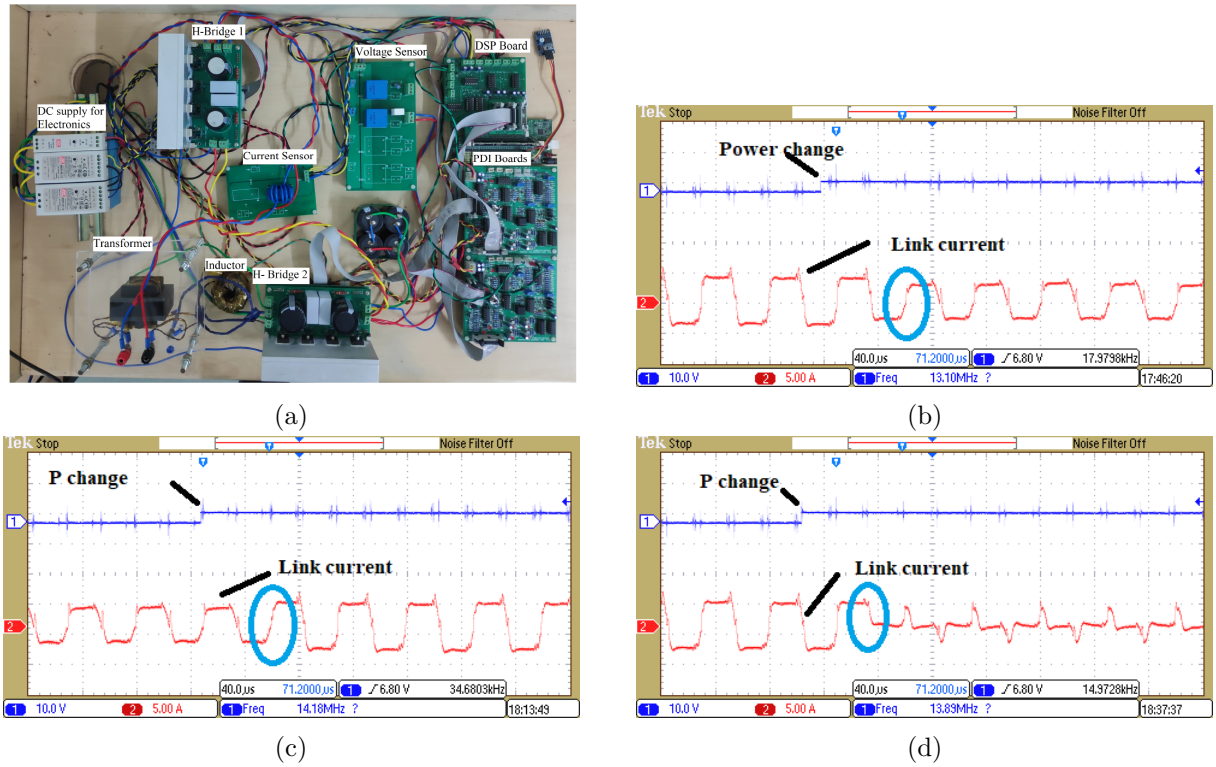

Fig. 7: (a) Photograph of the laboratory set up for DAB; (b) Experimental result of Link current (5A/div) with DPS: Transition from Case A -880W to Case B -730W, Time (20 μs/div); (c) Experimental result of Link current (5A/div) with DPS: Transition from Case B -730W to Case A -880W, Time (20 μs/div); (d) Experimental result of Link current (5A/div) with DPS: Transition from Case A-880W to Case E -50W, Time (20 μs/div)

2008.

[2] Tong A., Hang L., Li G., Jiang X. and Gao S.: Modeling and Analysis of a Dual Active-Bridge-Isolated Bidirectional DC/DC Converter to Minimize RMS Current with Whole Operating Range, IEEE Trans. Power Electronics, vol. 33, no. 6, pp. 5302-5316, June 2018.

[3] Bu Q., Wen H., Wen J., Hu Y., Du Y.: Transient DC Bias Elimination of Dual-Active-Bridge DC-DC Converter with Improved Triple-Phase-Shift Control, IEEE Trans. Industrial Electronics, vol. 67, no. 10, October 2020.

[4] Zhang Z., Sun J., Wang P., Cai Z., Kong J., Bai X., Ma D.: An Improved DC Bias Elimination Strategy with Extended Phase Shift Control for Dual-Active-Bridge DC-DC, CAC 2019, pp. 4274-4279.

[5] Bu Q., and Wen H., Control Strategies for DC-bias Current Elimination in Dual-Active-Bridge DC-DC Converter: An Overview, ICPS Asia 2020, pp. 1155-1162.

[6] Pena-Alzola R., Mathe L., Liserre M., Blaabjerg F. and Kerekes T.: DC-bias cancellation for phase shift controlled dual active bridge, IECON 2013, pp. 596-600.

[7] Zhao B., Song Q., Liu W. and Zhao Y.: Transient DC Bias and Current Impact Effects of High-Frequency-Isolated Bidirectional DC–DC Converter in Practice, IEEE Trans. Power Electronics, vol. 31, no. 4, pp. 3203-3216, April 2016.

[8] Takagi K. and Fujita H.: Dynamic Control and Performance of a Dual-Active-Bridge DC–DC Converter, IEEE Trans. Power Electron, vol. 33, no. 9, pp. 7858-7866, Sept. 2018.

[9] Su J., Luo S. and Wu F.: Improvement on Transient Performance of Cooperative Triple-Phase-Shift Control for Dual Active Bridge DC-DC Converter, ECCE 2019, pp. 1296-1301.

[10] Li Z., Wang Y., Shi L., Huang J., Lei W.: Optimized modulation strategy for three-phase dual-active-bridge DC-DC converters to minimize RMS inductor current in the whole load range, IPEMC-ECCE Asia 2016, pp. 2787-2791.

[11] Shi H., Wen H., Chen J., Hu Y., Jiang L. and Chen G.: Minimum-Reactive-Power Scheme of Dual-Active-Bridge DC-DC Converter with Three-Level Modulated Phase Shift Control, IEEE Trans. Industry Applications , vol. 53, no. 6, pp. 5573-5586, Nov.-Dec. 2017.

[12] Hu J., Yang Z. and De Doncker R. W.: A Comprehensive Dead Time Compensation Method for a Three-Phase Dual-Active Bridge Converter with Hybrid Modulation Schemes, IEEE IPEC, pp 1073 - 1079, 2018.
[13] Zhao B., Song Q., Liu W. and Sun Y.: Dead-Time Effect of the High-Frequency Isolated Bidirectional Full-Bridge DC-DC Converter: Comprehensive Theoretical Analysis and Experimental Verification, IEEE Trans. Power Electron., Vol. 29, No.4, pp.1667-1680, 2014.
[14] Takagi K. and Fujita H.: Dynamic Control and Dead-Time Compensation Method of an Isolated Dual-Active-Bridge DC-DC Converter,IEEE ECPA 2015, pp-1-10.
[15] Luo S., Wu F. and Gang W.: Effect of Dead Band and Transient Actions on CTPS Modulation for DAB DC-DC Converter and Solutions, IEEE Trans. on Transportation Electrification, vol. 7, no. 4, pp. 949-957.
[16] Mukherjee S., Dash A., De D. and Castellazzi A.: Study of Dual Active Bridge with Modified Modulation Techniques for Harmonic Reduction in AC Link Current, ICSETS 2019, pp. 144-149.
[17] Maharana S., Mukherjee S., De D. and Castellazzi A.: Dead-Time Compensated Dual Active Bridge with Online Hybrid Optimized Operation, ICPEE 2021, pp. 1-6.
[18] Mukherjee S., Dash A., De D. and Castellazzi A.: Trade-off in Minimization of Fundamental Link Current and Reactive Power using a Novel Online Calculation based Triple Phase Shift Modulator for Dual Active Bridge, EPE ECCE Europe 2019, pp. P.1-P.10